An Updated Quantification Method for Liquid Refrigerant Distribution in Microchannel Evaporators Using Infrared Thermography

Yuping Gao
Creative Thermal Solutions Inc

Daniel Silsbee
Creative Thermal Solutions Inc

Ke Tang
Creative Thermal Solutions Inc, ke.tang@creativethermalsolutions.com

Stefan Elbel
Creative Thermal Solutions Inc

An Updated Quantification Method for Liquid Refrigerant Distribution in Microchannel Evaporators Using Infrared Thermography

Yuping GAO[1], Daniel SILSBEE[1], Ke TANG[1,2,*], Stefan ELBEL[1,2]

[1]Creative Thermal Solutions, Inc.,
Urbana, Illinois, USA
yuping.gao@creativethermalsolutions.com

[2] University of Illinois at Urbana-Champaign, Mechanical Science and Engineering,
Urbana, Illinois, USA
ketang@illinois.edu

* Corresponding Author

ABSTRACT

Refrigerant distribution in the parallel tubes of a microchannel evaporator significantly affects its heat transfer performance, which can further affect the coefficient of performance of the whole air-conditioning or refrigeration system. This paper proposes an easy-to-implement quantification method using infrared thermography for the liquid refrigerant distribution in microchannel evaporators to update the original method developed by Li and Hrnjak (2015). Before the detailed discussion of the new quantification method, the effect of surface emissivity on the infrared thermography is investigated, and the calibration process of the infrared thermography is presented for a microchannel heat exchanger sample. Then, the updated quantification method is introduced in detail. The *ε-NTU* approach is clarified for the formula derivation. A new mathematical method is introduced for the determination of the transition between the two-phase region and the single-phase region. A facility with pump-driven two-phase refrigerant R134a has been built to demonstrate the updated quantification method for the liquid refrigerant distribution in a microchannel evaporator with vertical parallel tubes. The tests have been run at the conditions of 41.7 g/s refrigerant flow rate and 5 ºC evaporation temperature with the evaporator inlet vapor quality of 0.15 and 0.25, respectively. The infrared images and the reduced liquid refrigerant mass flow rate distributions are presented to demonstrate the effectiveness of the updated quantification method.

1. INTRODUCTION

Microchannel heat exchanger (MCHX) is a compact and efficient heat exchanger, which is widely used as an evaporator or a condenser in air-conditioning and refrigeration systems. Since parallel tubes are employed in the MCHXs, refrigerant distribution in the parallel tubes significantly affects its heat transfer performance, which can further affect the coefficient of performance of the whole air-conditioning or refrigeration system (Byun and Kim, 2011; Hrnjak, 2004; Lee, 2009; Shi *et al*., 2011; Tuo and Hrnjak, 2013). In the microchannel evaporators, the refrigerant usually enters the inlet header as two-phase. Therefore, the two-phase flow regime in the inlet header is a dominant factor that affects the refrigerant distribution in the parallel tubes of the microchannel evaporator. Considering the complexity of the two-phase flow modeling, the analytical or numerical methods to predict the refrigerant distribution in microchannel evaporators are still challenging.

Infrared thermography is a non-intrusive method to get the surface temperature of an object, which has the advantage of time and cost-saving. The infrared thermography can be used to easily get the wall temperature distribution of a microchannel evaporator. Li and Hrnjak (2015) linked the wall temperature distribution with the liquid refrigerant distribution in the parallel tubes of the microchannel evaporator and finally developed a quantitative method. In this study, several updates have been performed to the original method developed by Li and Hrnjak (2015). The *ε-NTU* approach is clarified for the formula derivation. A new mathematical method is introduced for the determination of the transition between the two-phase region and the single-phase region. Furthermore, a facility with pump-driven two-phase refrigerant R134a has been built to demonstrate the updated quantification method for the liquid refrigerant distribution in a microchannel evaporator with vertical parallel tubes.

2. EFFECT OF EMISSIVITY ON INFRARED THERMOGRAPHY AND CALIBRATION

The emissivity of a material surface is the effectiveness of emitting energy as thermal radiation. The temperature and emissivity of the surface determine its thermal radiation. In other words, the temperature of a surface can be determined by detecting and quantifying its thermal radiation with a known emissivity. The emissivity of a surface can vary from 0 to 1, depending on its material and surficial micro-structure. For instance, the emissivity of a shiny mirror is almost 0 and that of a flat black painted surface is close to 1. In such circumstances, the calibration for the emissivity of the target surface is the first step for determining its temperature with infrared thermography.

The microchannel heat exchanger is usually made of aluminum alloy, which is a kind of conductor. The emissivity of conductors is not constant but increases with temperature (Bergman *et al*., 2011). Additionally, the surface emissivity of a given material is also affected by the method of fabrication, thermal cycling, and chemical reaction with its environment. On the other hand, when taking the infrared images, the camera usually receives not only the radiation emitted by the target surface itself but also the radiation which is emitted by the surroundings and reflected by the target surface. The preceding discussion presents the difficulty in the determination of the emissivity of the original MCHX surface. A possible solution is to coat the aluminum surface with a thin layer of flat black paint. The flat black paint coating is supposed to give an emissivity close to 1 and a reflectivity close to 0.

In order to verify the effectiveness of the flat black paint coating, a piece of MCHX sample is prepared with half of the surface coated. A setup is designed to perform the infrared thermography calibration on the MCHX surface, as shown in Figure 1. The MCHX sample is embedded into a wind tunnel. A hairdryer is employed to provide different operating temperatures. Two thermocouples are attached on the same microchannel tube within the unpainted zone and the painted zone, respectively. The thermocouples are thermal insulated to ensure that the wall temperature is measured.

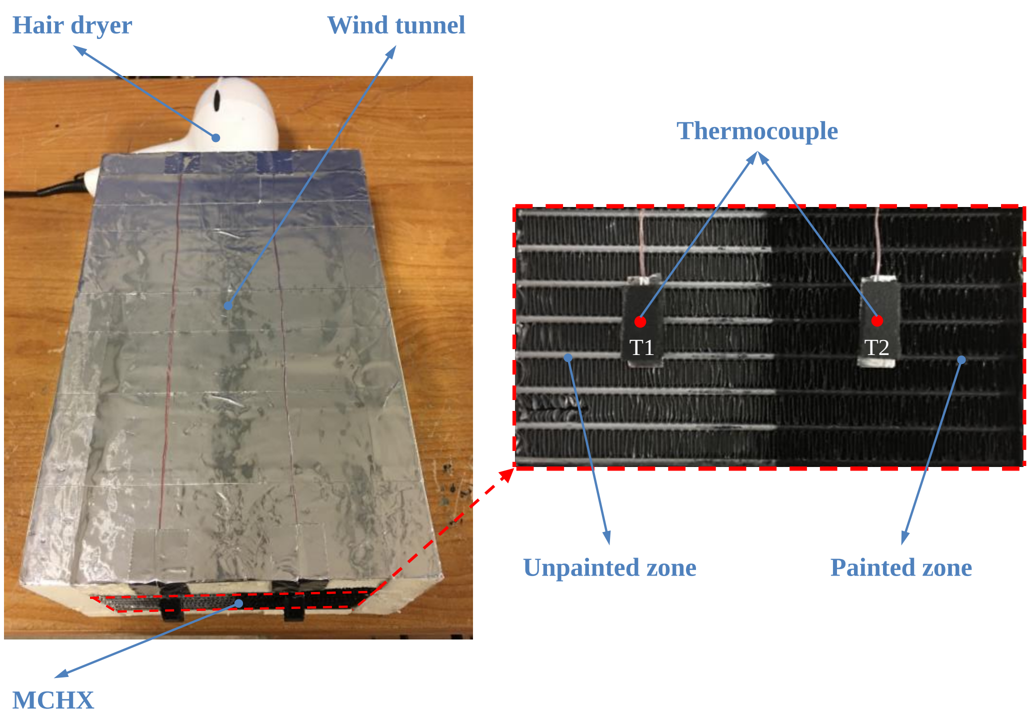

Figure 1: Setup for infrared thermography calibration

Two cases with different operating temperatures have been tested. The infrared images (the emissivity is set to 1) together with the thermocouple readings are presented in Figure 2. It can be seen that the difference in thermocouple readings for each case is within 0.1 ºC, indicating a uniform temperature profile on the microchannel tube. However, the temperatures indicated by the infrared images are visibly different for the unpainted and painted zones, which is attributed to the different emissivities. The temperature profiles from the infrared thermography on the microchannel tube where the thermocouples are attached for the two cases are extracted, as shown in Figure 3. The two red solid lines correspond to the thermocouple locations. Because the infrared thermography at this location is for the thermal insulation surface rather than the microchannel tube surface, the temperature readings on the same microchannel tube within the two dash lines next to the thermocouples are used for the calibration.

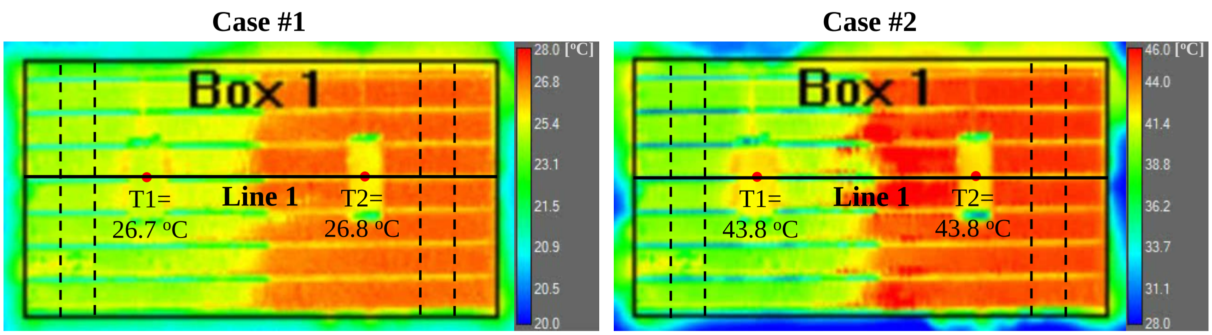

Figure 2: Infrared images of MCHX sample in two cases with different operating temperatures

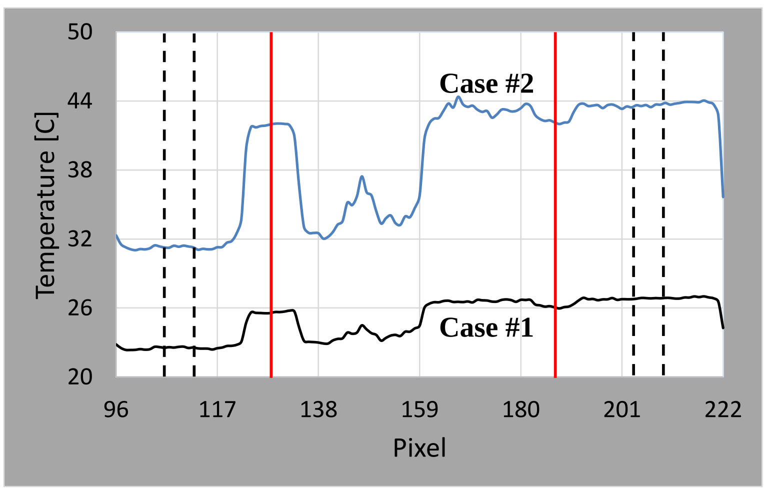

Figure 3: Temperature profiles on line 1 from infrared thermography with emissivity set as 1 for two cases with different operating temperatures

The reduced emissivities for the unpainted surface and the painted surface are presented in Table 1 and Table 2, respectively. The emissivity of the unpainted surface (the original MCHX surface) is indeed increased with increasing temperature. Whereas the painted surface has an almost constant emissivity and closes to 1. That means the flat black paint coating makes the surface act like a black body. Therefore, the surface of the MCHX for detecting the thermal radiation in this study is coated with flat black paint to keep the emissivity constant and to eliminate the effect of reflection.

Table 1: Emissivity determination for unpainted surface

Case	Thermocouple reading, T1 [ºC]	Infrared thermography reading with $\varepsilon = 1$, T_IR [ºC]	Emissivity, ε [-]
#1	26.7	22.5	0.360
#2	43.8	31.3	0.446

Table 2: Emissivity determination for painted surface

Case	Thermocouple reading, T2 [ºC]	Infrared thermography reading with ε = 1, T_IR [ºC]	Emissivity, ε [-]
#1	26.8	26.8	1.000
#2	43.8	43.7	0.995

3. UPDATED QUANTIFICATION METHOD FOR LIQUID REFRIGERANT DISTRIBUTION IN MICROCHANNEL EVAPORATORS

The original quantification method was developed by Li and Hrnjak in 2015. In this paper, the *ε-NTU* approach is clarified for the formula derivation. Besides, a new mathematical method is proposed for the determination of the transition between the two-phase region and the single-phase region. The updated quantification method is introduced in detail in this section.

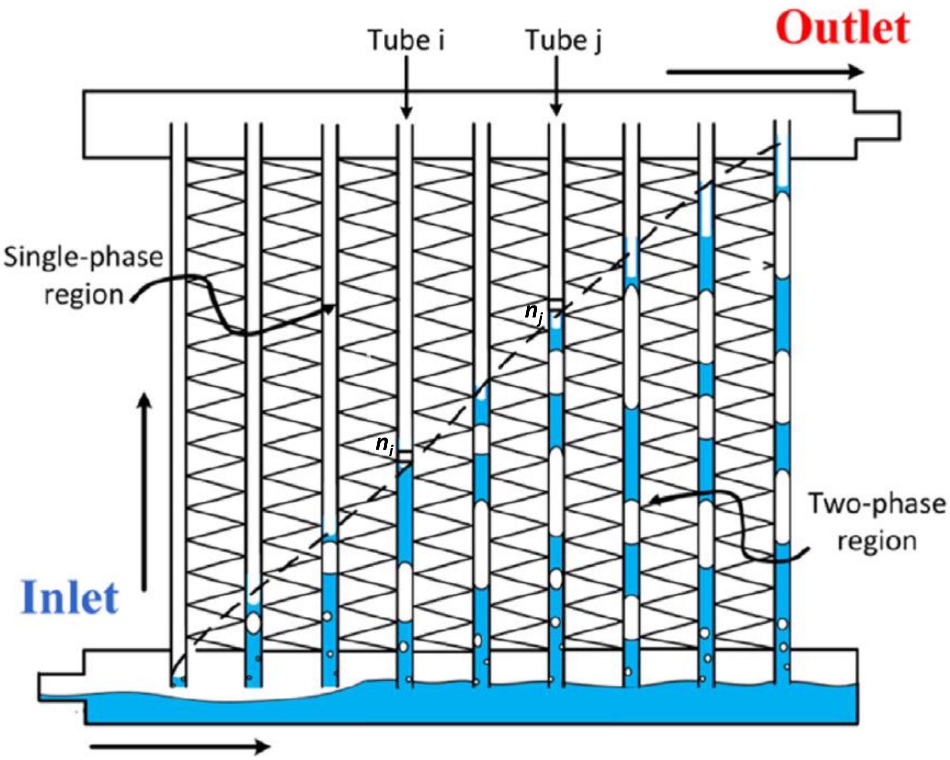

Figure 4: Schematic of a simplified situation in microchannel evaporator (Li and Hrnjak, 2015)

A schematic of a simplified situation in a microchannel evaporator is shown in Figure 4. The microchannel evaporator has several parallel microchannel tubes, and each tube is divided into elements. Assuming dry condition (no condensation or frosting on the air-side) for the microchannel evaporator, applying the *ε-NTU* approach for each element, we get

$$NTU = \frac{KA}{c_{p,a}\dot{m}_a}, \tag{1}$$

$$\varepsilon = \frac{T_{a,i}-T_{a,o}}{T_{a,i}-T_{r,i}}, \tag{2}$$

where K is the overall heat transfer coefficient between the refrigerant and air, A is the heat transfer area, $c_{p,a}$ and $\dot{m}_a$ are the constant-pressure specific heat and mass flow rate of air, $T_{a,i}$ and $T_{a,o}$ are the air inlet and outlet temperatures, and $T_{r,i}$ is the refrigerant inlet temperature. For the element with refrigerant evaporating inside the tube, ε is given by

$$\varepsilon = 1 - \exp(-NTU). \tag{3}$$

The refrigerant-side capacity mainly comes from the latent heat of the liquid refrigerant which undergoes evaporation. Therefore, in the two-phase region, the refrigerant-side capacity in an element can be illustrated as

$$dQ_r = h_{lv} d\dot{m}_{r,l}, \tag{4}$$

where h_{lv} is the latent heat of the refrigerant, and $\dot{m}_{r,l}$ is the mass flow rate of the liquid refrigerant. Assuming the latent heat of the refrigerant is constant and the outlet of the tube is superheated vapor, the refrigerant-side capacity for a signal tube within the two-phase region is integrated as

$$Q_r = h_{lv} \dot{m}_{r,l}. \tag{5}$$

For the dry condition, the air-side capacity in an element is calculated as

$$dQ_a = c_{p,a} \dot{m}_a \left(T_{a,i} - T_{a,o}\right) = \varepsilon c_{p,a} \dot{m}_a \left(T_{a,i} - T_{r,i}\right). \tag{6}$$

Assuming the overall heat transfer coefficient K in the two-phase region is a constant and the mass flow rate distribution of the incoming air is uniform with constant specific heat, the air-side capacity for a signal tube within the two-phase region is integrated as

$$Q_a = \varepsilon c_{p,a} \dot{m}_a \sum_1^n \left(T_{a,i} - T_{r,i}\right), \tag{7}$$

where n is the number of elements in the two-phase region of that signal tube. Considering the heat balance between the refrigerant-side and air-side capacities, we get

$$h_{lv} \dot{m}_{r,l} = \varepsilon c_{p,a} \dot{m}_a \sum_1^n \left(T_{a,i} - T_{r,i}\right). \tag{8}$$

Then, the ratio of the liquid refrigerant mass flow rate through any two microchannel tubes can be calculated as follows

$$\frac{(\dot{m}_{r,l})_i}{(\dot{m}_{r,l})_j} = \frac{\left[\sum_1^{n_i} (T_{a,i} - T_{r,i})\right]_i}{\left[\sum_1^{n_j} (T_{a,i} - T_{r,i})\right]_j}, \tag{9}$$

where n_i and n_j are the numbers of the elements in the two-phase region for tubes i and j. Assuming uniform temperature of the incoming air, and uniform refrigerant saturation temperature in the two-phase region, Equation (9) can be further simplified as

$$\frac{(\dot{m}_{r,l})_i}{(\dot{m}_{r,l})_j} = \frac{n_i}{n_j}. \tag{10}$$

Given the above ratio, the liquid refrigerant distribution among parallel microchannel tubes can be fully described by Equation (11) as

$$\frac{(\dot{m}_{r,l})_i}{\dot{m}_{r,l,tot}} = \frac{n_i}{\sum_1^m n_i}, \tag{11}$$

where $\dot{m}_{r,l,tot}$ is the total liquid refrigerant mass flow rate in the entire heat exchanger, and m is the number of tubes. Using Equation (11), a relationship is built between the liquid mass flow rate through each microchannel tube and the corresponding number of elements in the two-phase region. An infrared camera is employed to provide the wall temperature measurement of each element. As long as the boundary between the single-phase region and the two-phase region (i.e. the transition line) is identified on the infrared image of the heat exchanger, the distribution of liquid refrigerant mass flow rate can be determined.

Figure 5(a) is an infrared image for a microchannel evaporator with vertical parallel tubes. The heat exchanger zone for heat transfer with air is indicated as "HX zone" in the infrared image. In the HX zone, there are 170 pixels vertically, which corresponds to the number of elements in a single microchannel tube. The methodology to determine the transition line is presented here with Figure 5 as an example. Along the upward flow direction in this image, the variation in the wall temperatures indicates that the heat exchanger can be divided into three regions corresponding to the three typical situations of the refrigerant flowing inside the tubes, i.e. the two-phase developing flow before the dryout, the dryout flow, and the superheated flow, respectively. The real transition line from two-phase flow to single-phase flow should be the boundary between dryout flow and superheated flow. However, if the transition line is determined in this way, the liquid refrigerant in the dryout region is accounted too much due to the sharply reduced heat transfer coefficient in this region. Therefore, an advisable transition line should be in a proper location within the dryout region. In order to explore the advisable transition line, the variation of the tube-averaged wall temperature along the flow direction is given in Figure 5(b). In the dryout region, the temperature at the location with the highest temperature growth rate is regarded as the transition temperature. Then, the isotherm of the transition temperature is determined as the transition line, as shown in Figure 6.

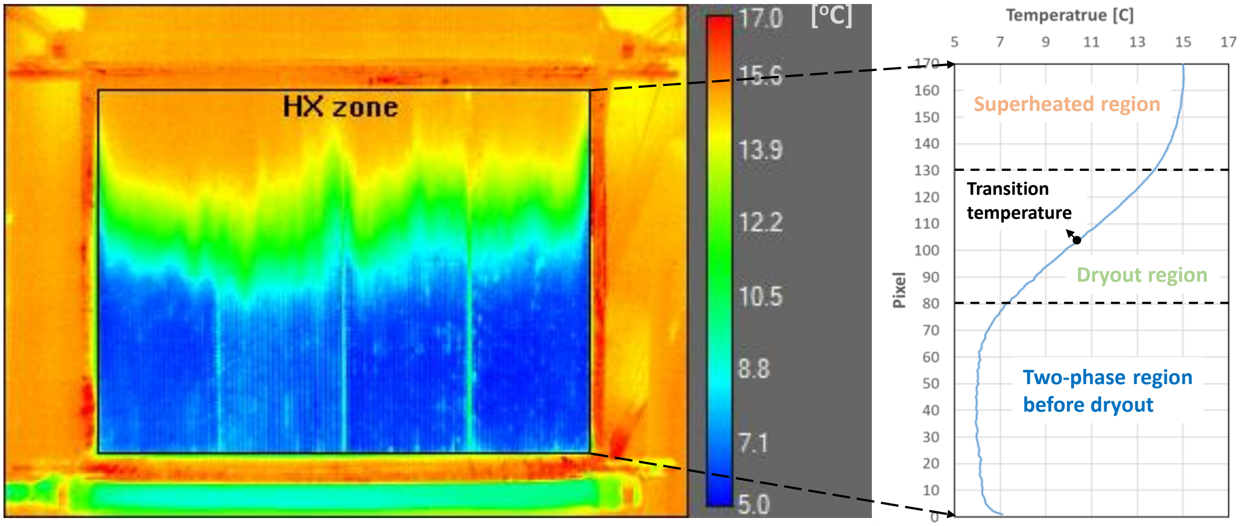

(a) (b)

Figure 5: Methodology to determine the transition line

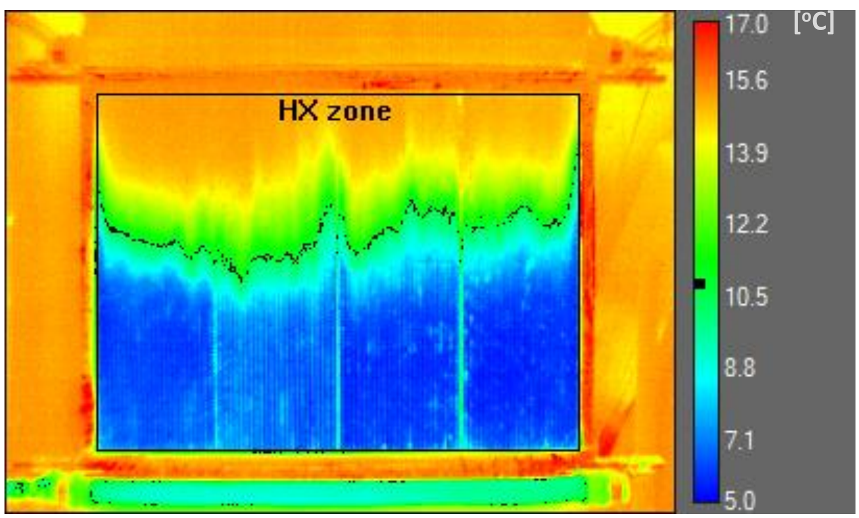

Figure 6: Infrared image with the transition line

4. APPLICATION OF THE UPDATED QUANTIFICATION METHOD

To demonstrate the updated quantification method for the liquid refrigerant distribution in a real microchannel evaporator with parallel tubes, a facility with pump-driven two-phase refrigerant R134a has been built. The tests have been run at the conditions of 41.7 g/s refrigerant flow rate and 5 ºC evaporation temperature with the evaporator inlet vapor quality of 0.15 and 0.25, respectively. The infrared images with the transition lines for the two cases are shown in Figures 7 and 8. The reduced liquid refrigerant mass flow rate distributions by using Equation (11) for the two cases are presented in Figures 9 and 10. It can be seen that the updated quantification method is capable to give fair liquid refrigerant distributions among the parallel microchannel tubes for the two cases.

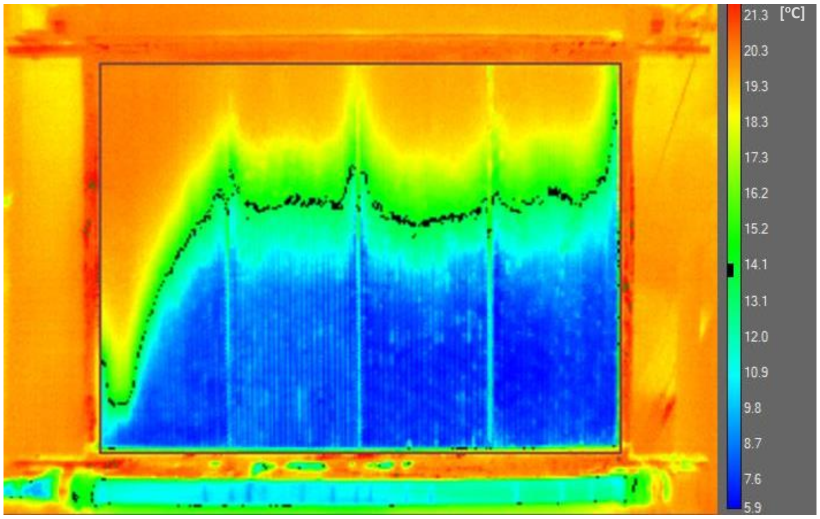

Figure 7: Infrared image with transition line with m = 41.7 g/s, T_{sat} = 5 °C, and x = 0.15

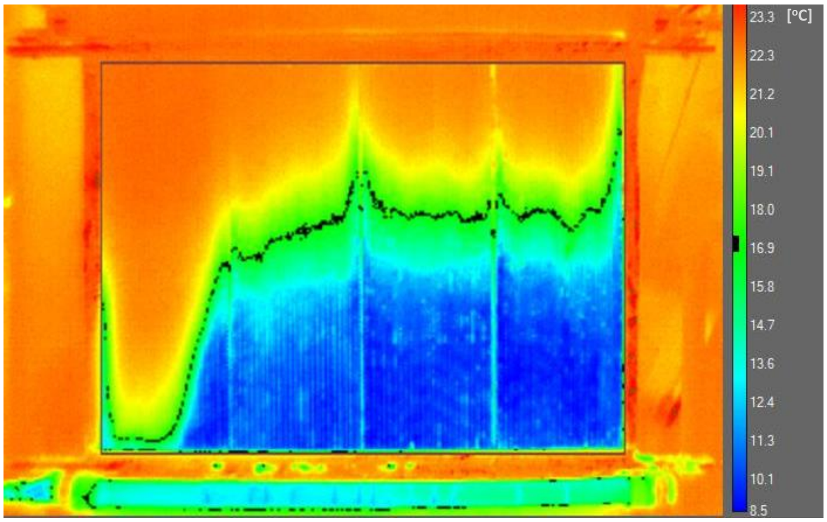

Figure 8: Infrared image with transition line with m = 41.7 g/s, T_{sat} = 5 °C, and x = 0.25

5. CONCLUSIONS

This study focuses on updating the quantification method for liquid refrigerant distribution in microchannel evaporators using infrared thermography. The calibration of the infrared thermography for its application on the surface temperature measurement of the MCHX is presented in detail. The ε-NTU approach is clarified for the formula derivation and a new mathematical method is proposed for the determination of the transition between the two-phase region and the single-phase region. At last, the updated quantification method is demonstrated in two cases with different operating conditions for a real microchannel evaporator. The results show that the updated quantification method can export fair liquid refrigerant distributions among the parallel microchannel tubes.

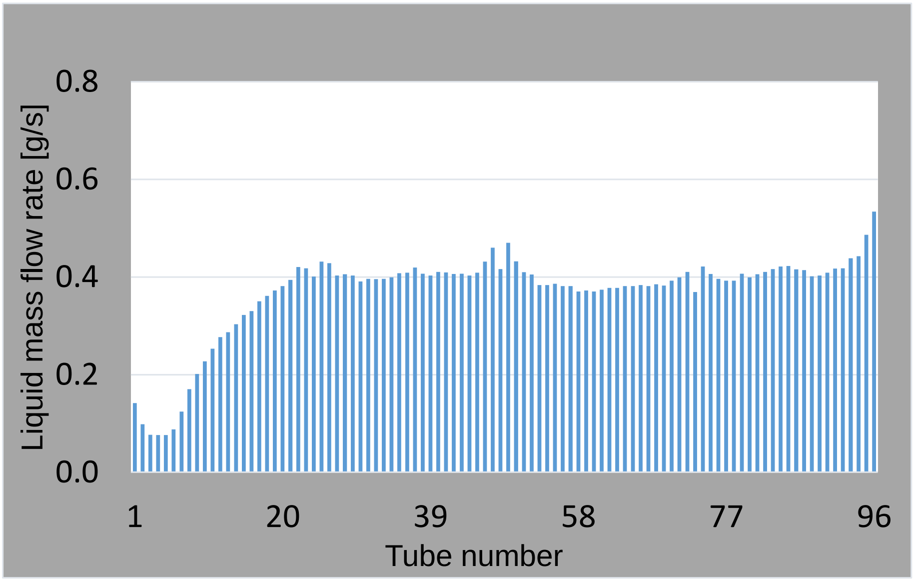

Figure 9: Liquid refrigerant distribution among parallel tubes with m = 41.7 g/s, T_{sat} = 5 °C, and x = 0.15

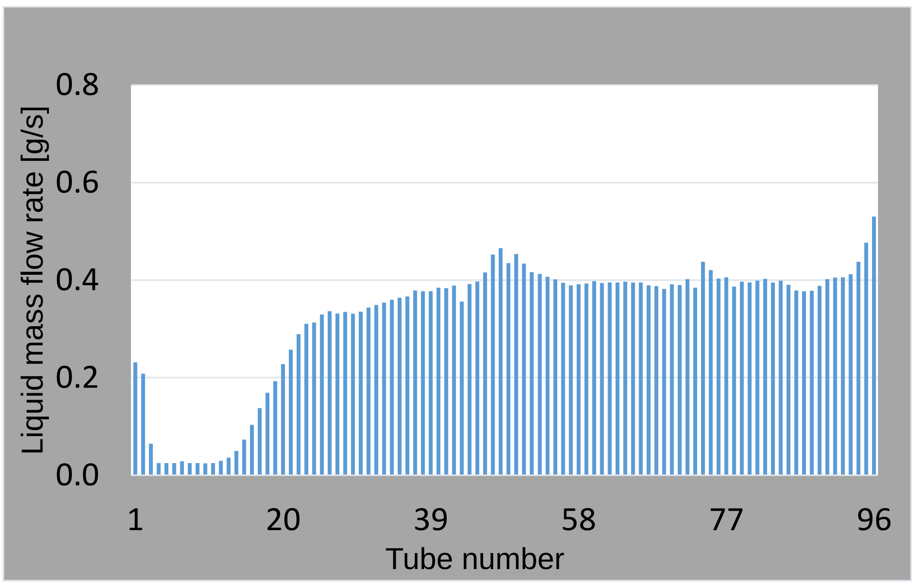

Figure 10: Liquid refrigerant distribution among parallel tubes with m = 41.7 g/s, T_{sat} = 5 °C, and x = 0.25

REFERENCE

Bergman, T. L., Incropera, F. P., DeWitt, D. P., & Lavine, A. S. (2011). Fundamentals of heat and mass transfer, pp. 795. John Wiley & Sons.

Byun, H. W., & Kim, N. H. (2011). Refrigerant distribution in a parallel flow heat exchanger having vertical headers and heated horizontal tubes. *Experimental Thermal and Fluid Science*, 35(6), 920-932.

Hrnjak, P. (2004). Developing adiabatic two phase flow in headers—distribution issue in parallel flow microchannel heat exchangers. *Heat Transfer Engineering*, 25(3), 61-68.

Lee, J. K. (2009). Two-phase flow behavior inside a header connected to multiple parallel channels. *Experimental Thermal and Fluid Science*, 33(2), 195-202.

Li, H., & Hrnjak, P. (2015). Quantification of liquid refrigerant distribution in parallel flow microchannel heat exchanger using infrared thermography. *Applied Thermal Engineering*, 78, 410-418.

Shi, J., Qu, X., Qi, Z., & Chen, J. (2011). Investigating performance of microchannel evaporators with different manifold structures. *International Journal of Refrigeration*, 34(1), 292-302.

Tuo, H., & Hrnjak, P. (2013). Effect of the header pressure drop induced flow maldistribution on the microchannel evaporator performance. *International journal of refrigeration*, 36(8), 2176-2186.